To cite this article: YE L Y, WANG C, SUN C, et al. Mathematical expression method for geometric shape of toroidal propeller [J/OL]. Chinese Journal of Ship Research, 2024, 19(3). http://www. ship-research. com/en/article/doi/10.19693/j.issn.1673-3185.03419 (in both Chinese and English).

DOI: 10.19693/j.issn.1673-3185. 03419

Mathematical expression method for geometric shape of toroidal propeller

YE Liyu[1], *WANG Chao*[*2], *SUN Cong*[2], *GUO Chunyu*[1]

1 Qingdao Innovation and Development Base, Harbin Engineering University, Qingdao 266400, China

2 College of Shipbuilding Engineering, Harbin Engineering University, Harbin 150001, China

Abstract: [**Objectives**] The toroidal propeller can effectively reduce tip vortex leakage due to its unique shape, which is beneficial for reducing hydrodynamic noise and improving propulsion efficiency. However, its complex shape also makes it challenging to model its geometric shape using conventional mathematical expression methods. Therefore, it is necessary to study the mathematical expression of the toroidal propeller. [**Methods**] First, the structural characteristics and advantages of the toroidal propeller are introduced in detail. Next, by referring to the mathematical expression of conventional propeller geometry, geometric parameters such as axis span, lateral angle, roll angle and vertical angle are introduced, and a detailed 3D coordinate formula for the toroidal propeller is derived by distributing the geometric parameters in the axis span direction, thereby establishing the mathematical expression method for toroidal propellers. Finally, by taking the offset of a certain toroidal propeller as an example, the feasibility of the proposed mathematical expression method for toroidal propellers is verified. [**Results**] The results show that the proposed method can smoothly establish the geometric shape of a toroidal propeller. [**Conclusions**] The proposed method can facilitate the rapid 3D modeling of toroidal propellers, laying a solid foundation for further research on the physical characteristics and scientific problems associated with toroidal propellers.

Key words: offset parameter; mathematical expression; reference line; geometric shape; toroidal propeller

CLC number: U664.33

0 Introduction

The implementation of the national strategy "carbon peaking and carbon neutrality" and the new regulations of energy conservation and emissions reduction issued by the International Maritime Organization (IMO) has added unprecedented urgency to the demand for developing energy-saving and emission-reducing vessels as well as actively promoting green shipping. In addition, the strategic transformation of the navy has put forward higher requirements on the overall performance of ships and underwater armament to support the modernization and upgrading of the naval equipment of China. The progressiveness of underwater propulsor technology directly determines the performance of ships and underwater vehicles in speed, endurance, and stealth. Conventional propellers, which are limited in the upgrading of propulsion capacity and noise control, can hardly meet the operational demands of ships and underwater vehicles in complex and variable marine environments. In recent years, the emergence of new, efficient, and low-noise toroidal propellers has attracted widespread attention. The unique external shape design of the toroidal propeller can reduce vortex shedding from the blade tips, thereby improving propulsion efficiency and lowering hydrodynamic noise. However, technical challenges and development bottlenecks also stem from its special shape. The complex and variable configuration of the toroidal propeller can hardly be modeled and designed using the mathematical expression methods for conventional propellers, which inhibits the industry from conducting in-depth fundamental research and is not conducive to the design and development of toroidal propellers. Therefore, further research should be conducted on the mathematical expression of the geometric shape of the new toroidal propeller.

Received: 2023 – 06 – 25 **Accepted**: 2023 – 08 – 09

***Corresponding author**: WANG Chao

For centuries, conventional propellers have been the main propulsion methods in the air and underwater. However, conventional propellers still have some unresolved drawbacks, such as the bottlenecks in improving propulsion efficiency and reducing hydrodynamic noise. In recent years, toroidal propellers have garnered widespread attention due to their potential to enhance propulsion efficiency and reduce vibration and noise, with research and applications in the maritime field already underway abroad. In 2013, Sharrow Marine in the United States filed a patent for their toroidal propeller [1] and developed a marine propulsor, claiming that it could improve the propulsion efficiency of vessels and reduce noise [2]. In 2017, the Massachusetts Institute of Technology (MIT) updated it and applied for another patent, which was approved in 2020 [3]. However, toroidal propellers have rarely been explored in China.

A reliable modeling method is a prerequisite for researching scientific issues related to toroidal propellers. However, the mathematical expression and modeling methods for the geometric shape of toroidal propellers are still unavailable, which limits the study and development of this equipment. To achieve breakthroughs in the key technologies for geometrically modeling toroidal propellers, the authors intend to study the mathematical expression methods for toroidal propellers. For this purpose, they start by detailing the structural characteristics and advantages of toroidal propellers. Then, drawing on the mathematical expression of the geometric shape of conventional propellers, they propose a mathematical expression method for the geometric shape of toroidal propellers, thereby rapidly and accurately modeling toroidal propellers three-dimensionally and providing a foundation for subsequent research on their physical properties and mechanisms of action.

1 Overview of toroidal propellers

The toroidal propeller consists of blades and a hub, with each blade being a closed annular structure that includes a front section, a transition section, and a rear section (Fig. 1). The transition section connecting the front and rear sections allows the blade to smoothly transition from the front section to the rear section. Despite no clear boundaries between these three sections on the blades, their positions can be roughly determined by observing the characteristics of the cure of roll angle distribution along the axial span. Generally, the roll angle increases slowly in the front and rear sections and rapidly in the transition section [1]. The point where the front section meets the hub is defined as the root of the front section, where the roll angle is 0°; the point where the rear section connects to the hub is defined as the root of the rear section, where the roll angle is 180°. Setting the roll angles at the front and rear roots to 0° and 180°, respectively, ensures that the points on the blade section are all located on the coaxial cylindrical surfaces with equal radii. The profile in the transition section with a radius of R is referred to as the tip, where the roll angle is approximately 90°.

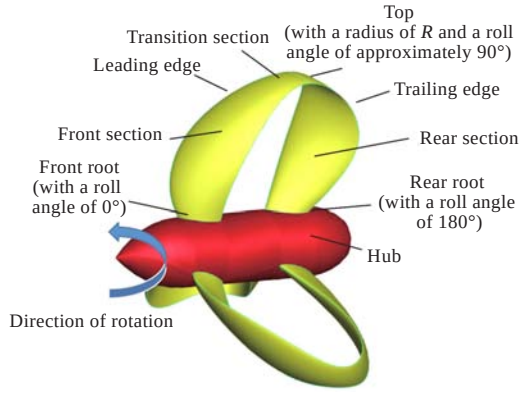

Fig. 1 Schematic diagram of the toroidal propeller

An observation of the characteristics of the geometric shape of the toroidal propeller reveals that it combines the advantages of the tandem propeller and the contracted and loaded tip (CLT) propeller.

A tandem propeller is a type of propulsor that has two conventionally shaped propellers mounted on the same shaft and rotating in the same direction simultaneously. The arrangement of one propeller in the front and the other in the rear with a particular interval places the rear propeller in the wake of the front one and thus gives it a higher advance speed. Therefore, the rear propeller typically has a larger pitch than that of the front one to enhance propulsion efficiency. For vessels with restricted diameters or excessive loads, tandem propellers can be used to conveniently increase the blade area, thereby reducing the load per unit area on the blade surface [4]. Consequently, the application of tandem propellers is beneficial for improving efficiency and avoiding or mitigating noise, cavitation, and vibration. The overall performance of tandem propellers is influenced not only by the same geometric parameters as those of conventional propellers but also

by the axial space (the axial span between the front and rear propeller discs) and the blade spacing angle (the angle by which the front blades lead the adjacent rear ones) [5]. Likewise, the propulsion performance of toroidal propellers is affected by the distance and stagger angle between the front and rear sections since the two sections are similar to the front and rear propellers of a tandem propeller.

For an airfoil with a finite span, a vortex that rolls inward, known as a tip vortex, usually forms at the ends of the wings due to the pressure difference between the upper and lower surfaces of the wings [6]. Tip vortices degrade the propulsion efficiency and noise performance of vessels, consequently limiting ship designers' choices of propellers' geometric parameters. Tip vortex suppression is thus one of the most common problems and challenges facing propeller designers. CLT propellers, also known as tip-loaded propellers, are a type of propeller with end plates at the tips of the blades. The end plates typically bend either forward or backward to eliminate or reduce the vortex shedding from the blade tips, thereby significantly lowering ship noise and excitation forces as well as improving propulsion efficiency [7]. For this reason, the shape of the ends directly affects the propulsion performance of the vessel and the control of tip vortices. The transition section of toroidal propeller blades can approximately be regarded as a part composed of the forward-and backward-bending end plates at the blade tips of the CLT propeller; however, the smooth transition issue also deserves proper consideration, and the shape of the transition section also influences propulsion performance and tip vortex control.

The toroidal propeller is a quieter and more efficient propeller design. Different from conventional propeller blades, each toroidal propeller blade curves from the front root to the rear root, constituting a closed annular structure. This enclosed design significantly reduces vortices and the rotational resistance generated by the transition section, thereby improving propulsion efficiency and reducing noise. Compared with conventional propellers, the toroidal propeller distributes the generated vortices across the entire blade rather than just in the transition section, ultimately significantly reducing tip cavitation and minimizing the hydrodynamic noise in the cases with and without cavities. Additionally, the annular shape of the toroidal propeller increases its stiffness and stability, which is conducive to enhancing the overall strength. The Lincoln Laboratory of MIT and Sharrow Marine conducted research based on this concept and designed several marine toroidal propellers collaboratively [8], including the Sharrow MX™, Sharrow CX-1™, and Sharrow NX™ (Fig. 2).

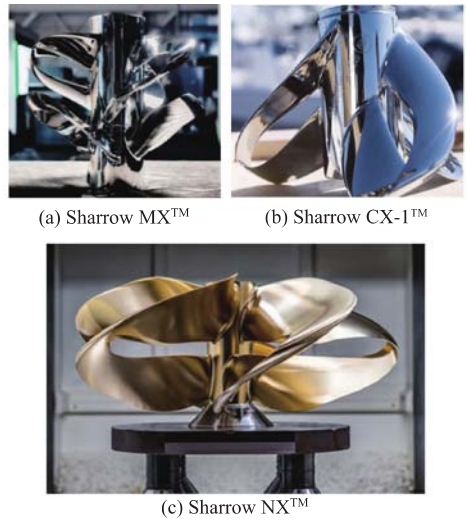

(a) Sharrow MX™ (b) Sharrow CX-1™

(c) Sharrow NX™

Fig. 2 Marine toroidal propellers from Sharrow Marine [8]

2 Mathematical expression of geometric shape of conventional propeller

Currently, a wealth of literature is available for mathematical expression methods for the geometric parameters and shapes of conventional propellers[9-10]. Only the reference curves for their geometric features and coordinate transformation equations will be discussed here. Assuming that the propeller rotates in place, the rotating coordinate system fixed to the propeller is defined as (x, r, θ). In this coordinate system, the x-axis coincides with the propeller axis, with the downstream direction as positive; r is the radial coordinate, with the outward direction as positive; θ is the coordinate in the angular direction, with the direction determined by the right-hand rule around the x-axis as positive (Fig. 3) [11].

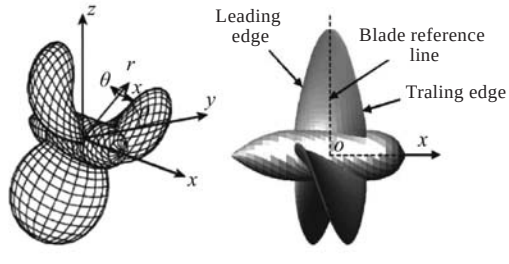

(a) Coordinate system (b) Reference line

Fig. 3 Coordinate system and reference line for conventional propeller [11]

The reference line for the propeller, defined as the radial line through the midpoint of the chord line of the blade root profile, is fixed to the propeller. A plane projected from this reference line and perpendicular to the *x*-axis is plotted, and the intersection point of this plane with the *x*-axis is then obtained and designated as the origin of coordinates. The blade reference plane is composed of constant-pitch reference helices distributed along the *r*-direction. The intersection line between the plane at $\theta = 0$ and the reference plane can be expressed as follows:

$$\begin{cases} x = x_r(r) \\ r = r \\ \theta = 0 \end{cases} \tag{1}$$

where x_r is the rake at the blade section. This curve is referred to as the blade generatrix and is used to depict the rake of the blade.

During the modeling of the propeller, a blade reference line must be defined so that other parameters can be arranged around it. The blade reference line is generally expressed as the following Eq. (2):

$$\begin{cases} x = x_{\mathrm{T}}(r) \\ r = r \\ \theta = \theta_{\mathrm{s}}(r) \end{cases} \tag{2}$$

where θ_{s} is the distribution of the skew angle; x_{T} is the total rake consisted of two parts: the rake of the blade itself, denoted as x_r, and that induced by the skew, and x_{T} can be expressed as follows:

$$x_{\mathrm{T}}(r) = x_r(r) + r\theta_{\mathrm{s}}(r)\tan\beta(r) \tag{3}$$

where β is the geometric pitch angle at a specific radius, indicating the inclination degree of the blade section at that radius. The relationships among the above reference lines can be found in Reference [11].

The position of a blade section in the three-dimensional space can be roughly depicted once the blade reference line is determined. However, additional parameters are required to determine the shape of the blade section, specifically its chord length *b* and form. The form of the profile can be calculated as the distances y_{h} from points on the blade section (including the coordinate points on the upper and lower surfaces of the profile) to the chord line, as shown in Fig. 4.

Typically, the skew shape of a propeller blade can be directly represented by the skew angle θ_{s} or by the distance c_1 from the leading edge to the generatrix of the blade section. If the former way is chosen, each point on the blade section at a radius *r* in the cylindrical coordinate system *o-xrθ* can be expressed as follows:

$$\begin{cases} x = x_{\mathrm{T}} + \left(-\dfrac{b}{2} + s\right)\sin\beta - \begin{pmatrix} y_{\mathrm{b}} \\ y_{\mathrm{f}} \end{pmatrix}\cos\beta \\ r = r \\ \theta = \theta_{\mathrm{s}} + \dfrac{1}{r}\left[\left(-\dfrac{b}{2} + s\right)\cos\beta + \begin{pmatrix} y_{\mathrm{b}} \\ y_{\mathrm{f}} \end{pmatrix}\sin\beta\right] \end{cases} \tag{4}$$

where *s* is the chordwise distance from the point on the blade section to the leading edge, while y_{b} and y_{f} are the distances from points on the blade back and blade face to the chord line, respectively.

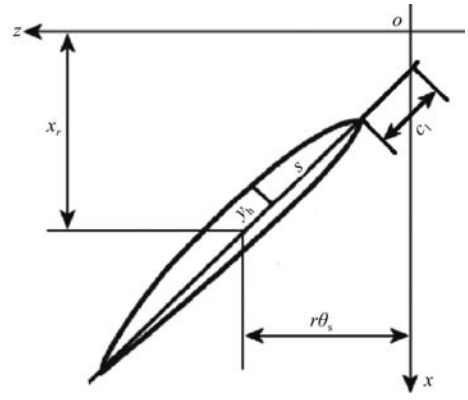

Fig. 4 Expression of blade section of conventional propeller

In the Cartesian coordinate system *o-xyz*, the coordinates of a point on the profile can be expressed as follows:

$$\begin{cases} x = x_{\mathrm{T}} + \left(-\dfrac{b}{2} + s\right)\sin\beta - \begin{pmatrix} y_{\mathrm{b}} \\ y_{\mathrm{f}} \end{pmatrix}\cos\beta \\ y = r\cos\theta \\ z = r\sin\theta \end{cases} \tag{5}$$

Eqs. (4) - (5) indicate that for a conventional propeller with given geometric elements (including its diameter, hub-radius ratio, number of blades, and its chord length, pitch, skew, backward leaning, and blade section distributed radially), the coordinate points on the propeller surface in the three-dimensional space can be determined by mathematical equations for three-dimensional coordinates (Eqs. (4) - (5)). Specifically, the coordinates of points on the blade back can be calculated by substituting y_{b} into the equations, while those of points on the blade face can be obtained by substituting y_{f} into the equations.

If the skew of the propeller is represented by the distance c_1, the points on the blade section at a radius *r* in the cylindrical coordinate system *o-xrθ* can be expressed as follows:

$$\begin{cases} x = x_r + (-c_1 + s)\sin\beta - \begin{pmatrix} y_b \\ y_f \end{pmatrix}\cos\beta \\ r = r \\ \theta = \dfrac{1}{r}\left[(-c_1 + s)\cos\beta + \begin{pmatrix} y_b \\ y_f \end{pmatrix}\sin\beta\right] \end{cases} \tag{6}$$

In the Cartesian coordinate system *o-xyz*, the coordinates of a point on the blade section can be expressed as follows:

$$\begin{cases} x = x_r + (-c_1 + s)\sin\beta - \begin{pmatrix} y_b \\ y_f \end{pmatrix}\cos\beta \\ y = r\cos\theta \\ z = r\sin\theta \end{cases} \tag{7}$$

A comparison between Eq. (4) and Eq. (6) suggests that the distance c_1 from the leading edge of the blade section to the generatrix can be obtained as follows:

$$c_1 = \frac{b}{2} - \frac{r\theta_s}{\cos\beta} \tag{8}$$

where the direction pointing from the leading edge to the trailing edge of the blade section is taken as positive for c_1. In Fig. 4, the distance c_1 from the leading edge to the generatrix points in the negative direction, indicating a negative c_1.

For a conventional propeller with given geometric elements (including its diameter, hub-radius ratio, number of blades, and its chord length, pitch, backward rake, distance from the leading edge to the generatrix, and the blade section distributed radially), the coordinate points on the propeller surface in the three-dimensional space can be determined using Eqs. (6)−(7), the mathematical equations for three-dimensional coordinates [12].

The above process can be implemented to determine the blade reference line first, whereby the positions of the blade sections at various radii in the three-dimensional space can be identified. Then, the blade section at each radius can be developed along the reference line to obtain the coordinates of all the points on the blade back and blade face in the three-dimensional space for the sections at different radii. This process completes the transformation of the propeller's offset parameters into coordinate points in the three-dimensional space through mathematical expressions.

3 Mathematical expression of geometric shape of toroidal propeller

The geometric offset parameters of conventional propellers include chord length, pitch, rake, skew (or the distance from the leading edge to the generatrix), as well as the camber and thickness of the blade airfoil sections. Each of these parameters varies with the radius, namely that they are functionally related to the radius. In comparison, the blades of a toroidal propeller are closed structures. When they are intersected by the cylindrical surface coaxial with the toroidal propeller, two blade sections are obtained. In this case, the same radius r corresponds to two geometric parametric variables in terms of the functional relationship. Therefore, the geometric offset parameters of a toroidal propeller can hardly be described as radially distributed.

To smoothly express the geometric shape of the toroidal propeller, the author introduced the concept of the axial span (Fig. 5). The position of the blade section at the front root was taken as the starting point, and the axial span l was then defined as the distance from each point on the reference line for the toroidal propeller to this starting point. The axial span between the front root and the rear root was defined as the total axial span L. In this case, each plane that covered the axial span l and was perpendicular to the x-axis would intersect with the reference line for the toroidal propeller at only one point. The geometric offset parameters can be set as functions that vary with the axial span to ensure their smooth curves of distribution along the axial span. In addition to the offset parameters required by the expression of conventional propellers, more parameters such as the lateral angle φ, roll angle ψ, and vertical angle α should also be introduced to express the toroidal propeller, which will be detailed later.

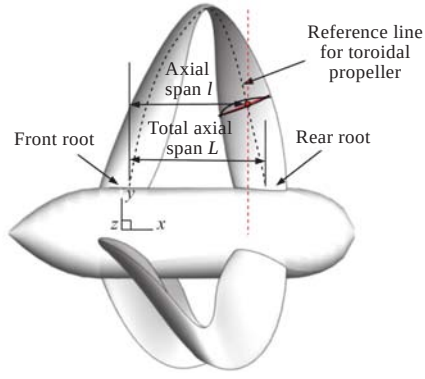

Fig. 5 Axis span and total axis span of toroidal propeller

A blade reference line should also be defined in the modeling of the toroidal propeller, as in the case of conventional propellers. Each blade section

develops around its blade reference line to form the three-dimensional model of the toroidal propeller. The blade reference line should be determined before mathematically expressing the geometric shape of the toroidal propeller. Assuming that the toroidal propeller rotates in place, the rotating coordinate system fixed on the toroidal propeller was denoted as (x, r, θ), as shown in Fig. 6. The intersection point of the radial line through the midpoint of the chord line of the front root profile with the x-axis was taken as the origin of the coordinates.

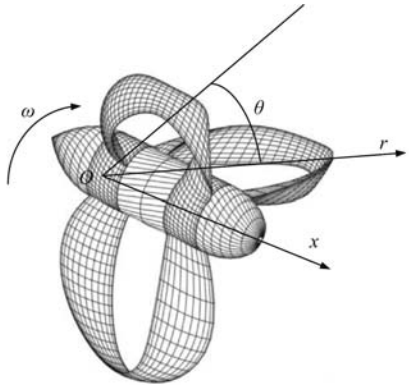

Fig. 6 Definition of coordinate system for toroidal propeller

For conventional propellers, the radial line through the midpoint of the chord line of the blade root profile is taken as the reference line, which is equivalent to the line connecting the points where blade sections at various radii are under the condition of no rake or skew. Similarly, in the case of the toroidal propeller, the curve formed as the radius varies with the axial span on the plane at θ = 0 can be used as the reference line since the toroidal propeller consists of closed annular structures. The reference line for the toroidal propeller can thus be expressed as follows:

$$\begin{cases} x = l \\ r = r_i(l) \\ \theta = 0 \end{cases} \tag{9}$$

where r_1 is the radius at the axial span l.

The axial span l varies in the axial direction and $l \in [0, L]$, and the curve varying with the axial span, namely, the reference line for the toroidal propeller, can be obtained from Eq. (9). Fig. 7 shows the front view and side view of the reference line for the toroidal propeller.

To increase or reduce the stagger angle between the front and rear sections of the toroidal propeller blades, the authors introduced the lateral angle $\varphi(l)$, which was defined as the angle by which the blade section rotates circumferentially. This angle can be represented by the angle between the radial line at the axial span l in the projected profile and the reference line for the toroidal propeller (Fig. 8), similar to the blade spacing angle between the front and rear blades of a tandem propeller. The front and rear sections of a toroidal propeller blade are separated by a particular gap, and the rear section is thus located in the wake of the front one. As a result, its advance speed is higher than that of the front section. Proper lateral angles should be chosen for the front and rear sections to achieve optimal propulsion efficiency matching. Generally, the lateral angles in the front and rear sections of a toroidal propeller are opposite, namely that the front section has a negative lateral angle while the rear section has a positive one. The transition section has a lateral angle transitioning from positive to negative. Fig. 8 illustrates an example where the lateral angle increases the stagger angle between the front and rear sections.

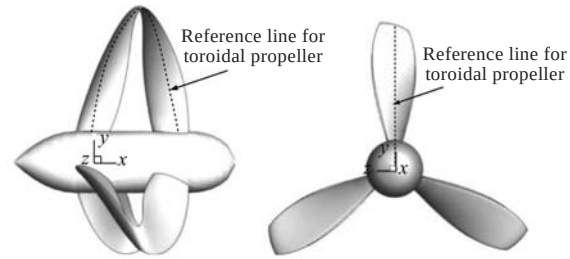

(a) Side view (b) Front view

Fig. 7 Reference line of toroidal propeller

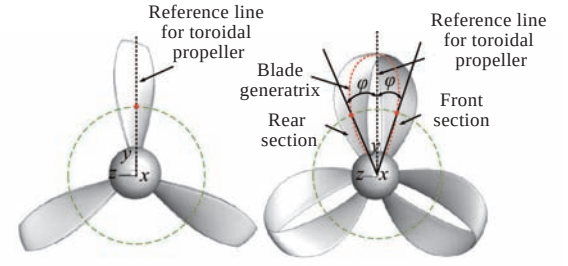

(a) Lateral angle out of consideration (b) Lateral angle in consideration

Fig. 8 Reference lines for toroidal propeller before and after lateral angle is considered

In the plane at θ = 0, the curve obtained by taking into consideration the effects of the rake $x_l(l)$ and the lateral angle $\varphi(l)$ on the basis of the reference line for the toroidal propeller was defined as the generatrix of the blade. Then, the generatrix of a toroidal propeller blade can be represented by Eq. (10) as follows:

$$\begin{cases} x = l + x_l(l) \\ r = r_l(l) \\ \theta = \varphi(l) \end{cases} \tag{10}$$

where x_l is the rake at the axis span l.

The curve varying with the axial span, namely, the blade generatrix of the toroidal propeller, can be obtained by Eq. (10) as the axial span l varies axially and $l \in [0, L]$ (Fig. 9).

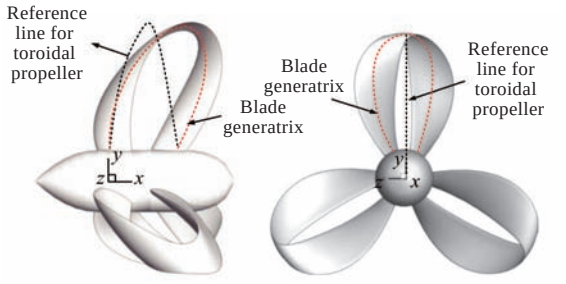

(a) Side view (b) Front view

Fig. 9 Blade generatrix of toroidal propeller

The midpoint of the chord line of the blade section at the axial span l can be expressed as follows:

$$\begin{cases} x = l + x_{\mathrm{T}}(l) \\ r = r_l(l) \\ \theta = \varphi(l) + \theta_{\mathrm{s}}(l) \end{cases} \tag{11}$$

where $\theta_{\mathrm{s}}(l)$ is the skew of the blade. The coordinate x in Eq. (11) is the sum of the axial span and the total rake x_{T}, namely that the blade sections at various axial spans are translated forward or backward along the x-axis relative to the propeller reference line. Similar to that in the case of conventional propellers, the total rake $x_{\mathrm{T}}(l)$ is composed of two parts and can be expressed as follows:

$$x_{\mathrm{T}}(l) = x_l(l) + r\theta_{\mathrm{s}}(l)\tan\beta(l) \tag{12}$$

where $r\theta_{\mathrm{s}}(l)\tan\beta(l)$ is the rake caused by the skew, referred to as the skew-induced axial displacement. Noteworthily, the skew $\theta_{\mathrm{s}}(l)$ and the lateral angle $\varphi(l)$ have different influences. To be specific, $\theta_{\mathrm{s}}(l)$ causes the blade section to rotate circumferentially and induces a rake along the axial direction simultaneously, while $\varphi(l)$ only causes the blade section to rotate circumferentially.

The curve varying with the axial span can be obtained by Eq. (12) as the axial span l varies in the axial direction and $l \in [0, L]$. This curve is defined as the blade reference line for the toroidal propeller, as shown in Fig. 10.

Similar to the mathematical expression method for conventional propellers, the mathematical expressions of the three-dimensional coordinates of the toroidal propeller can be obtained by determining the blade reference line first and then developing the blade section at each axial span l

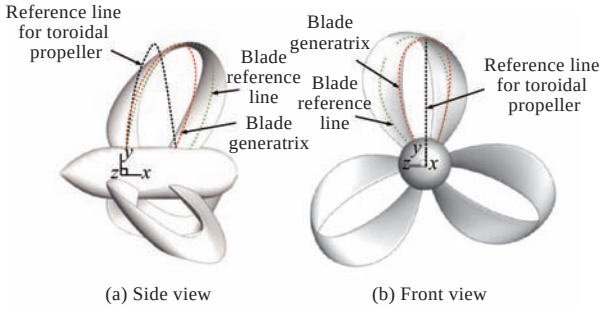

(a) Side view (b) Front view

Fig. 10 Blade reference line for toroidal propeller

along this reference line. In the cylindrical coordinate system o-$xr\theta$, the blade section at each axial span l of the toroidal propeller can first be developed around the blade reference line in the same manner as the blade sections of conventional propellers are processed. Then, preliminary mathematical expressions of the three-dimensional coordinates of the toroidal propeller can be obtained as follows:

$$\begin{cases} x = l + x_{\mathrm{T}} + \left(-\dfrac{b}{2} + s\right)\sin\beta - \begin{pmatrix} y_{\mathrm{b}} \\ y_{\mathrm{f}} \end{pmatrix}\cos\beta \\ r = r_l \\ \theta = \varphi + \theta_{\mathrm{s}} + \dfrac{1}{r}\left[\left(-\dfrac{b}{2} + s\right)\cos\beta + \begin{pmatrix} y_{\mathrm{b}} \\ y_{\mathrm{f}} \end{pmatrix}\sin\beta\right] \end{cases} \tag{13}$$

However, Eq. (13) still has a problem when it is used to express the geometric shape of the toroidal propeller: The total rake at the blade tip varies widely, which causes the distribution of the thickness of the transition section to differ significantly from that of the actual blade section (Fig. 11). Fig. 11 reveals that due to the excessive change in the curvature of the total rake in the transition section, the blade sections in this section becomes very thin, and the blade face even intersects with the blade back in the transition section ($r = R$), resulting in an intersection surface. Since the toroidal propeller is composed of closed structures, drastic changes in the total rake are inevitably observed at the blade tips, resulting in discrepancies between the thickness of the blade sections at these points and that in the actual

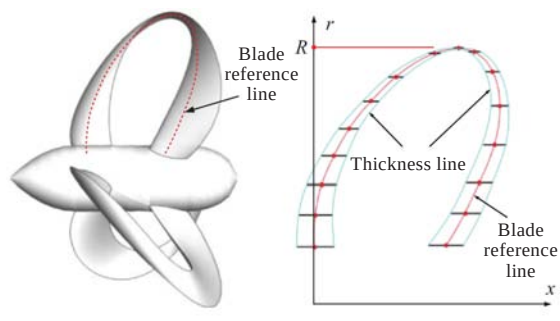

(a) Blade reference line (b) Thickness line

Fig. 11 Thickness of blade section before rotation

situation. Therefore, Eq. (13) alone is insufficient to fully and accurately express the geometric shape of the toroidal propeller.

The authors introduced the concept of the roll angle to ensure that each blade section of the toroidal propeller accurately reflects the actual thickness distribution. Its geometric definition is the angle between the tangent line to the blade reference line at the position of the blade section and the radial straight line, namely, the rotation angle of the blade section from a horizontal position to a position perpendicular to the blade reference line. Owing to the introduction of the blade section at each radius, a specified rotation angle can be freely chosen to ensure that the thickness of the blade tip is approximately equal to the thickness of the blade section. Additionally, the roll angle varies continuously among the front section, transition section, and rear section within the range of 0° – 180° to ensure the smoothness of the blades. The variation in the roll angle should be in tandem with the change in the total rake. In the front and rear sections of the blades, the roll angle does not need to vary widely due to the small change in the total rake. In the transition section, however, the variation in the roll angle should also be large due to the considerable change in the total rake. Fig. 12 shows the thickness lines of the toroidal propeller after the blade section is adjusted by the roll angle. Compared with the thickness lines in Fig. 11, the introduction of the roll angle enables the blade sections at different radii to reflect the thickness distribution of the blade more accurately.

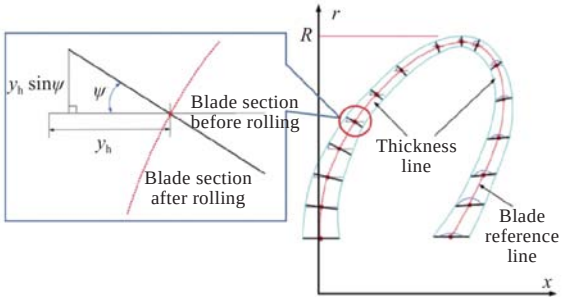

Fig. 12 Thickness of blade section after rotation

In the following part, the authors will detail how the roll angle is represented in the mathematical expressions of the three-dimensional coordinates of the toroidal propeller.

Fig. 12 can explain the change in the radial coordinate r in the mathematical expressions in Eq. (13). In Fig. 12, the fine black lines represent the position of the blade section at each axial span l before the blade section is adjusted by the roll angle, and all coordinate points on a specific blade section have a radius satisfying $r = r_l$. However, when the blade rotates to the specified roll angle, the radial coordinate r of points on the blade back and blade face increases or decreases by $-y_b\sin\psi$ and $-y_f\sin\psi$, respectively; namely that the radial coordinate r in Eq. (13) will change from $r = r_l$ to $r = r_l - (y_b\ y_f)\sin\psi$.

Fig. 13 shows the shapes of the blade section in the plane x-θ before and after the roll angle is considered. The cyan-green arcs in the figure are the contour of the blade section after it is adjusted by the roll angle. The changes in the axial coordinate x and the coordinate in the angular direction denoted as θ in the mathematical expressions in Eq. (13) can be explained by Fig. 13. From the perspective of the plane x-θ, Fig. 13 reveals that on the blade section at each axial span l, the coordinates of the points on the blade back and blade face perpendicular to the chord direction before rotation are y_b and y_f, respectively. After the blade section is rotated to the specified roll angle, their coordinates change to $y_b\cos\psi$ and $y_f\cos\psi$, respectively. This means that the $(y_b\ y_f)^T$ term in the calculation equations for x and θ in Eq. (13) changes to $\left[(y_b\ \ y_f)^T\cos\psi\right]$.

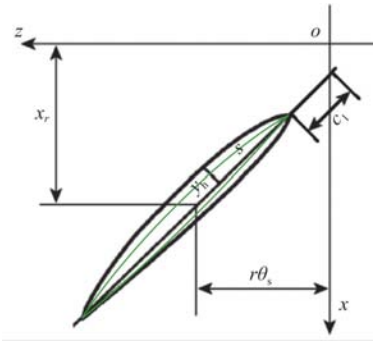

Fig. 13 Shapes of blade section before and after rolling

Therefore, in the cylindrical coordinate system o–$xr\theta$, the mathematical expressions of the three-dimensional coordinates in Eq. (13) will change to the following ones after the roll angle is added to the blade section at each axial span l:

$$\begin{cases} x = l + x_T + \left(-\dfrac{b}{2} + s\right)\sin\beta - \left[\begin{pmatrix} y_b \\ y_f \end{pmatrix}\cos\psi\right]\cos\beta \\ r = r_l - \begin{pmatrix} y_b \\ y_f \end{pmatrix}\sin\psi \\ \theta = \varphi + \theta_s + \dfrac{1}{r}\left\{\left(-\dfrac{b}{2} + s\right)\cos\beta + \left[\begin{pmatrix} y_b \\ y_f \end{pmatrix}\cos\psi\right]\sin\beta\right\} \end{cases} \quad (14)$$

In the absence of the roll angle, the angle of attack of the blade section is only influenced by the pitch. The introduction of the roll angle poses a problem, namely, the varying inflow conditions of the blade section at each axial span l on the blade (Fig. 14). In the figure, ω is the rotational angular velocity of the blade section, and ωr represents the rotational linear velocity of the blade section. The coordinate points on the blade sections at the front and rear roots of the blade are located on the section with the same radius. Therefore, the angle of attack of the inflow is mainly depend on the pitch at these points. In the vicinity of the transition section (where the roll angle is approximately 90°), the angle of attack of the inflow relies primarily on the angle between the chord line of the blade section on the plane r-θ and the direction of rotation of the blade section. As for blade sections at other axial spans, the angle of attack of the inflow is influenced not only by the pitch but also by the angle between the chord line and the direction of rotation.

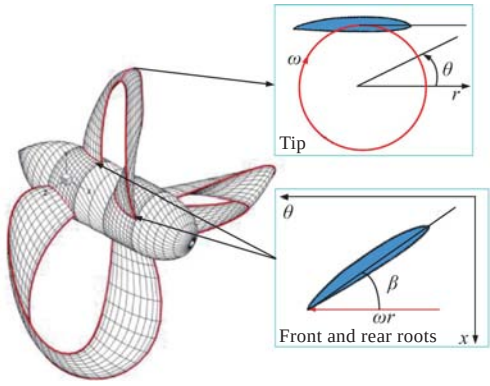

Fig. 14 Influence on angle of attack of inflow at different parts of toroidal propeller

The authors also introduced the vertical angle α to better adjust the angle of attack of the inflow on the blade sections so that the toroidal propeller can better adapt to the working environment. The geometric definition of the vertical angle is the angle between the chord line of the blade section and the rotation tangent (Fig. 15). The blade section can be lifted or lowered relative to the rotation tangent by adjusting the vertical angle. Adding the vertical angle to the transition section allows the fluid to be drawn into the interior of the blade "ring" but increases rotation resistance. Additionally, the vertical angle in the transition section also causes the fluid to deviate from the direction of the advance velocity. Therefore, the vertical angle of the rotating blade should be set properly. The vertical angle typically has three patterns of distribution along the axial span: 1) All blade sections have a vertical angle set to 0° ; 2) The vertical angle is positive in the front and transition sections and negative in the rear section; 3) All blade sections have a positive vertical angle, but the vertical angle is larger in the front and transition sections than in the rear section.

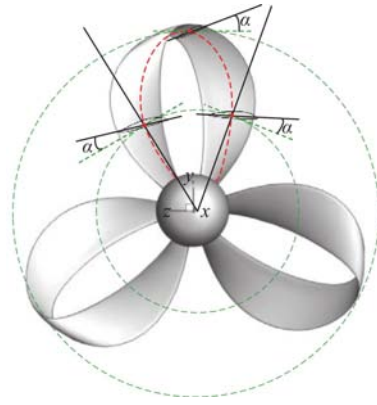

Fig. 15 Vertical angle of toroidal propeller

The representation of the vertical angle in the mathematical expressions of the three-dimensional coordinates of the toroidal propeller will be detailed in the following part.

The variation in the radial coordinate r in the mathematical expressions in Eq. (13) can be explained by Fig. 15. In the figure, the blue dashed line denotes the radius of the blade section at each axial span l before rolling, and $r = r_l$. When the blade section is rotated to the specified roll angle, it will be lifted or lowered in the direction of rotation, resulting in an increase or decrease in the radius r by $-(-c_1 + s)\sin\alpha$, namely that the radial coordinate r in Eq. (13) changes from $r = r_l$ to $r = r_l-(-c_1 + s)\sin\alpha$.

Fig. 16 shows the shapes of the blade section on the plane x-θ before and after the vertical angle is applied. In this figure, the cyan-green arcs are the contour of the blade section after it is adjusted by the vertical angle. The changes in the axial coordinate x and the coordinate in the angular direction denoted as θ in the mathematical expressions in Eq. (13) can be explained by Fig. 16. From the perspective of the plane x-θ, the length of the blade section at each axial span l in the chord line direction is $-b/2+ s$ before rotation. However, it becomes $(-b/2+ s)\cos\alpha$ after the blade section is rotated to the specified vertical angle, namely that the term $(-b/2+ s)$ in the calculation equations for x and θ in Eq. (13) changes to $[(-b/2+ s)\cos\alpha]$.

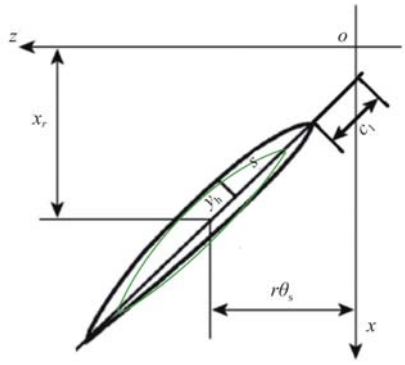

Fig. 16 Contour of blade section before and after vertical rotation

Therefore, in the cylindrical coordinate system $o-xr\theta$, the mathematical expressions of the three-dimensional coordinates in Eq. (13) change to the following ones after the vertical angle is applied to the blade section at each axial span l:

$$\begin{cases} x = l + x_T + \left[\left(-\dfrac{b}{2}+s\right)\cos\alpha\right]\sin\beta - \begin{pmatrix} y_b \\ y_f \end{pmatrix}\cos\beta \\ r = r_l - \left(-\dfrac{b}{2}+s\right)\sin\alpha \\ \theta = \varphi + \theta_s + \dfrac{1}{r}\left\{\left[\left(-\dfrac{b}{2}+s\right)\cos\alpha\right]\cos\beta + \begin{pmatrix} y_b \\ y_f \end{pmatrix}\sin\beta\right\} \end{cases} \tag{15}$$

In summary, the mathematical expressions of the three-dimensional coordinate points on the blade section at each axial span l in the cylindrical coordinate system $o-xr\theta$ are as follows after the axial span, the lateral angle, the roll angle, and the vertical angle are introduced into the case of the toroidal propeller:

$$\begin{cases} x = l + x_T + \left[\left(-\dfrac{b}{2}+s\right)\cos\alpha\right]\sin\beta - \left[\begin{pmatrix} y_b \\ y_f \end{pmatrix}\cos\psi\right]\cos\beta \\ r = r_l - \left(-\dfrac{b}{2}+s\right)\sin\alpha - \begin{pmatrix} y_b \\ y_f \end{pmatrix}\sin\psi \\ \theta = \varphi + \theta_s + \dfrac{1}{r}\left\{\left[\left(-\dfrac{b}{2}+s\right)\cos\alpha\right]\cos\beta + \right. \\ \qquad \left.\left[\begin{pmatrix} y_b \\ y_f \end{pmatrix}\cos\psi\right]\sin\beta\right\} \end{cases} \tag{16}$$

The three-dimensional coordinates of points on the blade section at each axial span l of the toroidal propeller in the Cartesian coordinate system $o-xyz$ can be expressed as follows:

$$\begin{cases} x = l + x_T + \left[\left(-\dfrac{b}{2}+s\right)\cos\alpha\right]\sin\beta - \left[\begin{pmatrix} y_b \\ y_f \end{pmatrix}\cos\psi\right]\cos\beta \\ y = r\cos\theta \\ z = r\sin\theta \end{cases} \tag{17}$$

Eqs. (16) − (17) indicate that for a toroidal propeller with given geometric parameters (including its total axial span, diameter, hub-radius ratio, number of blades, and its radius, chord length, pitch, skew, backward rake, and blade section distributed along the direction of its axial span), the coordinates of points on its surface in the three-dimensional space can be determined using the mathematical equations for the three-dimensional coordinates. Specifically, the coordinates of points on the blade back can be obtained by substituting y_b into the calculation equations, while those of points on the blade face can be obtained by substituting y_f into the equations.

Similar to the mathematical expressions of the three-dimensional coordinates of points for the geometric shape of conventional propellers, the points on the blade section at each axial span l can be expressed in the cylindrical coordinate system $o-xr\theta$ as follows if the distance c_1 from the leading edge to the generatrix of the blade section is used to express the geometric shape:

$$\begin{cases} x = l + x_l + [(-c_1+s)\cos\alpha]\sin\beta - \left[\begin{pmatrix} y_b \\ y_f \end{pmatrix}\cos\psi\right]\cos\beta \\ r = r_l - \left(-\dfrac{b}{2}+s\right)\sin\alpha - \begin{pmatrix} y_b \\ y_f \end{pmatrix}\sin\psi \\ \theta = \varphi + \dfrac{1}{r}\left\{[(-c_1+s)\cos\alpha]\cos\beta + \left[\begin{pmatrix} y_b \\ y_f \end{pmatrix}\cos\psi\right]\sin\beta\right\} \end{cases} \tag{18}$$

In this case, the three-dimensional coordinates of points on the blade section at each axis span l of the toroidal propeller in the Cartesian coordinate system $o-xyz$ can be expressed as follows:

$$\begin{cases} x = l + x_l + [(-c_1+s)\cos\alpha]\sin\beta - \left[\begin{pmatrix} y_b \\ y_f \end{pmatrix}\cos\psi\right]\cos\beta \\ y = r\cos\theta \\ z = r\sin\theta \end{cases} \tag{19}$$

The distance c_1 from the leading edge to the generatrix of the blade section can be determined as follows by comparing Eq. (16) with Eq. (18):

$$c_1 = \frac{b}{2} - \frac{r\theta_s}{\cos\beta\cos\alpha} \tag{20}$$

Eqs. (16)−(17) show that for a toroidal propeller with given geometric parameters (including its total axial span, diameter, hub-radius ratio, number of blades, and its radius, chord length, pitch, backward rake, distance from the leading edge to the generatrix, and blade sections distributed along the

direction of its axial span), the coordinates of points on the surface of the toroidal propeller in the three-dimensional space can be determined using the mathematical equations for the three-dimensional coordinates.

The above process involves first determining the blade reference line for the toroidal propeller, namely, the positions of the blade sections at various axial spans in the three-dimensional space. Then, the blade sections at different axial spans are developed along the blade reference line to obtain the coordinates of all points on the blade back and blade face of the toroidal propeller in the three-dimensional space. This process enables the authors to achieve the goal of converting offset parameters into the coordinates of points on the geometric shape in the three-dimensional space through mathematical expressions.

4 Application example

A program has been developed in FORTRAN to generate a three-dimensional model of the toroidal propeller by the abovementioned mathematical expression method for the toroidal propeller. This program can be operated to obtain the three-dimensional coordinate points on the blade sections at various axial span l on the premise of specified geometric parameters of the toroidal propeller (including its total axial span, diameter, hub-radius ratio, number of blades, and the distribution of its radius, chord length, pitch, thickness, rake, skew angle, or distance from the leading edge to the generatrix of the blade section, lateral angle, roll angle, vertical angle, and blade section along the axial span). These coordinate points can then be imported into three-dimensional software to fit the three-dimensional model of the toroidal propeller.

To verify the effectiveness of the mathematical expression method for the toroidal propeller proposed in this study, the authors examined the offsets of a specific toroidal propeller, whose parameters are listed in Tables 1 and 2. In Table 2, R is the propeller radius; P is the pitch distributed along the axial span; t is the thickness distributed along the axial span; f is the camber distributed along the axial span.

The three-dimensional coordinate points on the toroidal propeller are obtained by taking the offsets of the toroidal propeller in Tables 1 and 2 as inputs and running the program and shown in Fig. 17(a). The three-dimensional model of the toroidal propeller can then be easily constructed by three-dimensional modeling software, as illustrated in Figs. 17(b) −17(d). These figures demonstrate that the mathematical expression method for the toroidal propeller proposed in this study effectively facilitates the conversion from geometric offset parameters to smooth geometric shapes of the blades.

Table 1 Main parameters of toroidal propeller

Parameter	Value
Total axial span L/mm	160
Diameter D/mm	800
Hub-radius ratio r_h/R	0.2
Number of blade Z	3
Section form	NACA 66（mod）

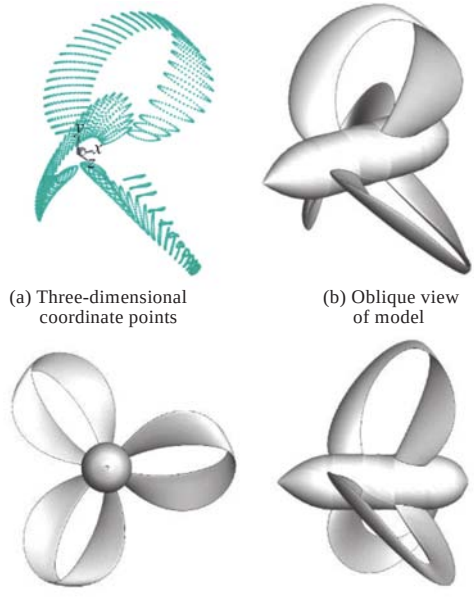

(a) Three-dimensional coordinate points (b) Oblique view of model

(c) Front view of model (d) Side view of model

Fig. 17 Three-dimensional coordinate points and model of toroidal propeller

5 Conclusions

This study investigated the mathematical expression method for the geometric shape of the toroidal propeller. Specifically, it provided the definitions of the coordinate system and reference lines for the toroidal propeller, as well as its blade generatrix and blade reference line. Then, it focused on the expression methods for geometric offset parameters such as the lateral angle, roll angle, and vertical angle in the mathematical equations for the three-dimensional coordinates of the toroidal propeller by setting geometric offset parameters to be variables along the direction of the axial span. Furthermore, a specific toroidal propeller was discussed as an

Table 2 Geometric parameters of toroidal propeller

l/L	r_l/R	b/D	P/D	t/b	f/b	θ_s /(°)	x_l/D	φ /(°)	ψ /(°)	α /(°)
0	0.200	0.121 0	1.312 0	0.300 7	0.014 0	0	−0.062 0	−27.56	0	0
0.062 4	0.300	0.143 1	1.331 1	0.243 3	0.030 4	−0.89	−0.082 2	−25.52	2.44	0.12
0.120 3	0.400	0.160 0	1.336 5	0.196 7	0.044 0	−1.10	−0.093 3	−23.44	3.38	0.62
0.177 3	0.500	0.172 3	1.320 6	0.157 6	0.055 0	−0.90	−0.096 8	−21.26	4.26	1.44
0.234 3	0.600	0.179 7	1.280 7	0.125 3	0.063 4	−0.36	−0.092 8	−18.93	5.44	2.61
0.293 7	0.700	0.180 6	1.198 0	0.098 6	0.068 9	0.43	−0.080 7	−16.33	8.31	4.37
0.359 0	0.800	0.168 3	1.078 4	0.077 4	0.069 8	1.46	−0.058 7	−13.26	14.67	6.89
0.437 7	0.900	0.142 3	0.931 7	0.060 8	0.061 9	2.83	−0.025 5	−9.33	28.78	9.39
0.488 9	0.950	0.122 8	0.863 1	0.054 8	0.051 8	3.78	−0.002 2	−6.55	42.83	10.45
0.525 0	0.975	0.112 0	0.830 0	0.052 6	0.043 1	4.45	0.014 0	−4.56	55.45	10.98
0.572 9	0.995	0.102 7	0.806 5	0.052 4	0.029 8	5.34	0.034 7	−1.86	75.91	11.41
0.600 0	1.000	0.101 0	0.806 0	0.053 8	0.021 6	5.87	0.045 8	−0.24	90.00	11.51
0.643 8	0.995	0.106 5	0.852 8	0.058 3	0.008 3	6.69	0.061 5	2.45	118.06	11.28
0.684 2	0.975	0.119 0	0.951 2	0.065 3	−0.003 5	7.44	0.073 2	4.99	139.40	10.52
0.714 6	0.950	0.131 1	1.040 0	0.072 7	−0.011 3	7.99	0.078 9	6.95	151.75	8.97
0.757 4	0.900	0.151 4	1.182 9	0.086 7	−0.020 3	8.75	0.081 9	9.78	164.02	5.54
0.815 0	0.800	0.176 3	1.395 9	0.113 8	−0.026 8	9.72	0.072 3	13.77	173.49	2.33
0.858 2	0.700	0.186 9	1.543 3	0.141 0	−0.027 6	10.40	0.053 7	16.83	176.68	1.44
0.894 1	0.600	0.186 2	1.636 7	0.168 6	−0.026 0	10.94	0.029 8	19.44	177.66	0.98
0.924 9	0.500	0.177 0	1.668 6	0.196 6	−0.023 0	11.39	0.002 4	21.74	178.50	0.63
0.952 3	0.400	0.162 6	1.663 6	0.224 6	−0.019 0	11.77	−0.027 2	23.82	179.13	0.38
0.977 1	0.300	0.144 7	1.652 4	0.252 6	−0.014 7	12.11	−0.058 4	25.74	179.62	0.17
1.000 0	0.200	0.124 0	1.631 0	0.280 7	−0.010 0	12.41	−0.091 0	27.56	180.00	0

example. The main conclusions obtained are as follows:

1) Given that the blades of the toroidal propeller are closed structures, the radial distribution of geometric parameters used to analyze conventional propellers is no longer applicable. Instead, geometric parameters should be distributed along the direction of the axial span, and three geometric parameters, namely, the lateral angle, roll angle, and vertical angle, should also be introduced so that the geometric shape of the toroidal propeller can be fully expressed.

2) The proposed mathematical expression method for the three-dimensional coordinates of toroidal propellers allows for the rapid calculation of coordinate points on the blade sections at different axial spans of a toroidal propeller by inputting geometric parameters and the further construction of a smooth three-dimensional geometric model of the toroidal propeller.

The proposed method can be applied to accurately express the geometric shape of a toroidal propeller and achieve quick three-dimensional modeling. Follow-up studies will be devoted to exploring the influence of geometric parameters on the performance of toroidal propellers in hydrodynamics, noise, and strength by applying the proposed method, revealing the underlying physical mechanisms and fluid dynamics principles underlying the performance of toroidal propellers, and providing support for the optimization design and performance improvement of toroidal propellers.

References

[1] SHARROW G C. Propeller: CN 108367801A [P]. 2018-08-03 (in Chinese).

[2] Boat Information. How do annular propellers affect aviation and navigation [EB/OL]. (2023-02-01) [2023-06-24]. https://baijiahao. bai du. com/s? id=1756593463110291574&wfr=spider&for=pc. Boat Information. How toroidal propellers affect the aviation and navigation industry[EB/OL]. (2023-02-01) [2023-06-24]. https://baijiahao. baidu. com/s? id=1756593463110291574&wfr=spider&for=pc (in Chinese).

[3] SEBASTIAN T, STREM C. Toroidal propeller: US, 10836466B2 [P]. 2020-11-17.

[4] WANG C, GUO C Y, CHANG X. Special propellers and additional rectification devices [M]. Harbin: Harbin Engineering University Press, 2013 (in Chinese).

[5] HU J M, LI T L, LIN Y, et al. Numerical simulation of the open water performance of parameter matching of B series tandem propellers [J]. Chinese Journal of Ship

Research, 2015, 10(5): 76−82 (in Chinese).
[6] JIANG L, CAI J G, LIU C Q. Large-eddy simulation of wing tip vortex in the near field [J]. International Journal of Computational Fluid Dynamics, 2008, 22 (5): 289−330.
[7] GAGGERO S, GONZALEZ-ADALID J, SOBRINO M P. Design of contracted and tip loaded propellers by using boundary element methods and optimization algorithms [J]. Applied Ocean Research, 2016, 55: 102−129.
[8] BLAIN L. Toroidal propellers: a noise-killing game changer in air and water [EB/OL]. New Atalas. (2023-01-26) [2023-06-24]. https://newatlas. com/aircraft/toroidal-quietpropellers/.
[9] WANG C. The research on performance of propeller's hydrodynamics, cavitation and noise [D]. Harbin: Harbin Engineering University, 2010 (in Chinese).
[10] SHENG Z B, LIU Y Z. Principles of ships (Part 2) [M]. Shanghai: Shanghai Jiao Tong University Press, 2004 (in Chinese).
[11] SU Y M, HUANG S. Ship propeller theory [M]. Harbin: Harbin Engineering University Press, 2003 (in Chinese).
[12] YE L Y, WANG C, HUANG S, et al. Multi-parameters optimization design of ship propeller based on multiobjective particle swarm algorithm [J]. Journal of Wuhan University of Technology (Transportation Science & Engineering), 2015, 39(6):1169−1174 (in Chinese).

环形螺旋桨几何形状的数学表达方法

叶礼裕[1], 王超[*2], 孙聪[2], 郭春雨[1]
1 哈尔滨工程大学 青岛创新发展基地, 山东 青岛 266400
2 哈尔滨工程大学 船舶工程学院, 黑龙江 哈尔滨 150001

摘　要: [**目的**] 环形螺旋桨因其独特的外形, 可有效减少梢涡泄出, 有利于降低水动力噪声, 提高推进效率, 但同时也因其复杂的外形, 难以采用常规螺旋桨的数学表达方法来对其几何外形进行建模, 因此, 需研究新型环形螺旋桨几何形状的数学表达。[**方法**] 首先, 详细介绍环形螺旋桨的结构特点和优势; 然后, 在参考常规螺旋桨几何形状数学表达的基础上, 引入轴距、外侧角、侧倾角和竖直角等几何参数, 以几何型值参数沿轴距方向分布的方式, 详细推导环形螺旋桨的三维坐标数学公式, 从而建立环形螺旋桨的数学表达方法; 最后, 以某一环形螺旋桨的型值为例, 验证所提环形螺旋桨数学表达方法的可行性。[**结果**] 结果显示, 采用所提方法能够光顺地建立环形螺旋桨的几何外形。[**结论**] 所提方法可用于快速进行环形螺旋桨的三维建模, 能为进一步研究环形螺旋桨的物理特性和科学问题奠定坚实的基础。

关键词: 型值参数; 数学表达; 参考线; 几何外形; 环形螺旋桨